ARTICLE IN PRESS

Available at
www.ElsevierComputerScience.com
POWERED BY SCIENCE DIRECT®

Signal Processing ▮ (▮▮▮▮) ▮▮▮–▮▮▮

SIGNAL PROCESSING

www.elsevier.com/locate/sigpro

Wavelet-based synthesis of the Rosenblatt process

Patrice Abry[a,*], Vladas Pipiras[b]

[a]CNRS UMR 5672, Ecole Normale Supérieure de Lyon, Laboratoire de Physique, 69364 Lyon Cedex 07, France
[b]Department of Statistics and Operations Research, Smith Building, CB #3260, University of North Carolina at Chapel Hill, Chapel Hill, NC 27599, USA

Received 8 March 2005; accepted 26 October 2005

Abstract

Based on a wavelet-type expansion of the Rosenblatt process, we introduce and examine two different practical ways to simulate the Rosenblatt process. The synthesis procedures proposed here are obtained by either truncating the series of the approximation term or using the approximation coefficients in the wavelet-type expansion of the Rosenblatt process. Both benefit from the low computational cost usually associated with the discrete wavelet transform. We show that the number of zero moments of a related orthogonal multiresolution analysis plays an important role. We study in detail the wavelet-based simulation in terms of uniform convergence. We also discuss at length the importance of the choices of the initial and final resolutions, the specific case of the simulation on the integer grid as well as the usefulness of the wavelet-based simulation. Matlab routines implementing these synthesis procedures as well as their analysis are available upon request.

Keywords: The Rosenblatt process; Long-range dependence; FARIMA sequence; Wavelet-type expansion; Low and high-pass filters; Zero moments; Simulation

1. Introduction

Our goal is to provide practical ways to simulate the Rosenblatt process by using wavelets, based on a wavelet-type expansion of the process established by Pipiras [1]. The *Rosenblatt process* $Z_\kappa(t)$, $t \in \mathbb{R}$, where $\kappa \in (\frac{1}{4}, \frac{1}{2})$ is a parameter, can be expressed as

$$Z_\kappa(t) = k_\kappa \int'_{\mathbb{R}^2} \left\{ \int_0^t (s-\xi_1)_+^{\kappa-1} (s-\xi_2)_+^{\kappa-1} \, \mathrm{d}s \right\} \times \mathrm{d}B(\xi_1)\, \mathrm{d}B(\xi_2), \tag{1.1}$$

where k_κ is a normalizing constant (e.g. such that $EZ_\kappa(1)^2 = 1$), $\int'_{\mathbb{R}^2}$ denotes the double Wiener-Itô integral (see, for example, [2]), $x_+ = \max\{x, 0\}$ for $x \in \mathbb{R}$ and $B(\xi)$, $\xi \in \mathbb{R}$, is a standard Brownian motion. We shall abbreviate throughout the Rosenblatt process as *fRm* (*fractional Rosenblatt motion*). FRm is *stationary increments* and (2κ)-*self-similar*. Self-similarity of Z_κ with the self-similarity parameter $2\kappa \in (\frac{1}{2}, 1)$ means that, for any $c > 0$,

$$\{Z_\kappa(ct)\}_{t\in\mathbb{R}} \stackrel{d}{=} \{c^{2\kappa} Z_\kappa(t)\}_{t\in\mathbb{R}}, \tag{1.2}$$

where the equality is in the sense of the finite-dimensional distributions (see, for example, [3] or Chapter 7 in [4]). The finite-dimensional distributions of fRm are non-Gaussian, have all their moments finite and their tails are heavier than those

*Corresponding author. Tel.: +33 47272 8493; fax: +33 47272 8080.
E-mail addresses: Patrice.Abry@ens-lyon.fr (P. Abry), pipiras@email.unc.edu (V. Pipiras).

0165-1684/$ - see front matter © 2005 Elsevier B.V. All rights reserved.
doi:10.1016/j.sigpro.2005.10.021

of the Gaussian distributions. In particular, fRm differs from the popular *fractional Brownian motion* (*fBm*, in short) which is the only Gaussian self-similar process with stationary increments. FRm was introduced by Rosenblatt [5], and also appears, for example, in Taqqu [6], Dobrushin and Major [7], Fox and Taqqu [8], and Embrechts and Maejima [3]. The asymptotic behavior of the right tail of $Z_\kappa(1)$ is derived in the proof of Theorem 2 [9, p. 88].

FRm is useful in applications as a self-similar process whose finite-dimensional distributions are non-Gaussian. For example, Monte Carlo simulations of its paths can be used to evaluate the performance of some estimator of a self-similarity parameter. FRm is also important in theory. Let X_k, $k \in \mathbb{Z}$, be a stationary, zero mean Gaussian time series with *long-range dependence* (see, for example, [10,11]), in the sense that its covariance function satisfies

$$EX_kX_0 = L(k)k^{\alpha-1} \quad \text{with } \alpha \in (0,1), \tag{1.3}$$

where L is a slowly varying function at infinity (e.g. $L(k)\sim$const, as $k \to \infty$; see Bingham et al. [12]). If

$$F(x) = x^2 - EX_0^2 \tag{1.4}$$

and $[x]$ denotes the integer part function of $x \in \mathbb{R}$, then

$$n^{-\alpha} \sum_{k=1}^{[nt]} F(X_k) \xrightarrow{d} Z_{\alpha/2}(t), \quad t \in \mathbb{R}, \tag{1.5}$$

where $\xrightarrow{d}$ stands for the weak convergence in the space of functions. The convergence (1.1) is a special case of the so-called *Non-Central Limit Theorem* (see [6,7,13,3]). Non-Central Limit Theorem concerns the limits of the partial sum $\sum_{k=1}^{[nt]} F(X_k)$ for more general functions F such that $EF(X_0)^2 < \infty$. The limit of these suitably normalized partial sums turns out to belong to the family of the *Hermite processes* where fBm and fRm are the Hermite processes of first and second order, respectively. The limit of the partial sums is fBm when, for example, $F(x) = x$.

Non-Central Limit Theorem shows that fRm can be obtained as the limit of the sums of square-like functions of long-range dependent sequences. Another standard connection to long-range dependence [3, p. 21] is that the increment sequence $Y_k = Z_\kappa(k+1) - Z_\kappa(k)$, $k \in \mathbb{Z}$, of (2κ)-self-similar fRm Z_κ is long-range dependent itself with $\alpha = 4\kappa - 1$.

We are interested here in simulation of fRm by using wavelets. We propose two approximations of fRm based on the *wavelet-type* expansion of the process established by Pipiras [1]. The first approximation uses the truncated series of the approximation term in the wavelet-type expansion. The second approximation does not involve truncation, and consists in using only the approximation coefficients in the expansion. Even though the wavelet-type expansion of fRm is non-standard, both of the proposed approximations are computed in practice by exploiting the usual fast wavelet transform. We describe below how the approximations are implemented and provide a number of practical guidelines to the simulation procedures. We argue, in particular, that the number of zero moments of a related orthogonal multiresolution analysis plays a fundamental role. We also discuss usefulness of the wavelet-based synthesis.

We will show that the second approximation, in fact, takes the form

$$2^{-2J\kappa} \sum_{k=1}^{[2^J t]} (Y_k^2 - EY_k^2), \tag{1.6}$$

where 2^{-J} is a desired approximation scale, and Y_k is a long-range dependent, the so-called FARIMA$(0,\kappa,0)$ time series. The approximation (1.6) is, therefore, equivalent to (1.5) with the function F in (1.4). The difference here is that Y_k itself is obtained through a wavelet-based method. The advantages and interest in generating Y_k by using wavelets, as opposed to other methods, are detailed in Section 7. Mainly, we will show that using wavelets leads to the convergence of (1.6) which is almost sure, uniform on compact intervals and exponentially fast, allows to study the rate of convergence and makes the synthesis of (1.6) computationally very fast.

The rest of the paper is organized as follows. In Section 2, we describe the two wavelet-based approximations of fRm. These approximations involve approximation coefficients and basis functions whose computation is explained in Section 3. In Section 4, we show how the wavelet-based approximations are implemented in practice. In Section 5, we provide some evidence for the uniform convergence of these approximations and their asymptotic equivalence. Discussion on use and usefulness of the wavelet-based synthesis of fRm can be found in Sections 6 and 7.

2. Two wavelet-based approximations

The proposed wavelet synthesis of fRm is based on the wavelet-type expansion of the process established by Pipiras [1]. We first recall the relevant notation and results of Pipiras [1]. Let ϕ and ψ be a *scaling function* and a *wavelet*, respectively, corresponding to an orthogonal *multiresolution analysis* (MRA, in short). Let the functions $\phi_{j,k}(u) = 2^{j/2}\phi(2^j u - k)$ and $\psi_{j,k}(u) = 2^{j/2}\psi(2^j u - k)$, $j,k \in \mathbb{Z}$, be their dilated and translated copies.

Define the function $\phi_{\kappa,\Delta}$ through its Fourier transformation as

$$\widehat{\phi}_{\kappa,\Delta}(x) = \left(\frac{1-\mathrm{e}^{-ix}}{ix}\right)^{\kappa}\widehat{\phi}(x), \quad x \in \mathbb{R}, \tag{2.1}$$

where $\widehat{f}(x) = \int_{\mathbb{R}} \mathrm{e}^{-\mathrm{i}xu} f(u)\,\mathrm{d}u$ (supposing that (2.1) is well-defined). For $n \in \mathbb{Z}$, set

$$\Phi^{(2)}_{\kappa,n}(z) = \int_{z-1}^{z} \phi_{\kappa,\Delta}(v)\phi_{\kappa,\Delta}(v-n)\,\mathrm{d}v, \quad z \in \mathbb{R}. \tag{2.2}$$

Let also $\xi_{j,k} = \int_{\mathbb{R}} \phi_{j,k}(\xi)\,\mathrm{d}B(\xi)$, $\varepsilon_{j,k} = \int_{\mathbb{R}} \psi_{j,k}(\xi)\,\mathrm{d}B(\xi)$, $j,k \in \mathbb{Z}$, be the random variables defined by using the standard Brownian motion $B(\xi)$, $\xi \in \mathbb{R}$, appearing in (1.1). Since ϕ and ψ correspond to an orthogonal MRA, the random variables $\xi_{J,k}$ and $\varepsilon_{j,k}$, $k \in \mathbb{Z}, j \geqslant J$, are independent Gaussian $\mathcal{N}(0,1)$. For a fixed j, define also the sequence

$$\xi^{(\kappa)}_{j,k} = (I-B)^{-\kappa}\xi_{j,k} = \sum_{l=0}^{\infty} \gamma_l^{(-\kappa)}\xi_{j,k-l}, \quad k \in \mathbb{Z}, \tag{2.3}$$

where $\gamma_l^{(-\kappa)}$ are the coefficients in the Taylor expansion of the function $(1-z)^{-\kappa}$ at $z=0$, B is the standard backshift operator. The series defined by (2.3) is a well-known long-range dependent FARIMA$(0,\kappa,0)$ sequence [14,10]. For $n,k,j \in \mathbb{Z}$, set also

$$S^{(\kappa,2)}_{k,n}(j) = \sum_{0<i\leqslant k} (\xi^{(\kappa)}_{j,i}\xi^{(\kappa)}_{j,i+n} - E\xi^{(\kappa)}_{j,i}\xi^{(\kappa)}_{j,i+n}), \tag{2.4}$$

where $\sum_{0<i\leqslant k} = 0$ if $k=0$, and $\sum_{0<i\leqslant k} = -\sum_{k<i\leqslant 0}$ if $k \leqslant -1$.

As shown in Theorem 1 of Pipiras [1], under suitable conditions on the scaling and wavelet functions ϕ and ψ:

Wavelet-based approximation I: We have

$$\sup_{t\in K} |Z_\kappa(t) - Z_{\kappa,1}(j,t)| \to 0, \quad \text{a.s. as } j \to \infty, \tag{2.5}$$

where K is a compact subset of $\mathbb{R}$, "a.s." stands for "almost surely", and

$$Z_{\kappa,1}(j,t) = 2^{-2\kappa j}\sum_{k=-\infty}^{\infty}\sum_{n=-\infty}^{\infty} \Phi^{(2)}_{\kappa,n}(2^j t - k) \times S^{(\kappa,2)}_{k,n}(j) - z_0^{(j)}, \tag{2.6}$$

with $z_0^{(j)}$ such that $Z_{\kappa,1}(j,0) = 0$.

The process $Z_{\kappa,1}(j,\cdot)$ defines an approximation of fRm Z_κ at scale 2^{-j} with the *approximation coefficients* and the *basis functions*

$$S^{(\kappa,2)}_{k,n}(j) \quad \text{and} \quad \Phi^{(2)}_{\kappa,n}, \tag{2.7}$$

respectively. The conditions for the convergence (2.5) are satisfied, for example, by the functions ϕ and ψ corresponding to the Daubechies, Meyer and other commonly used MRAs.

Another wavelet-based approximation of fRm uses only the approximation coefficients in the wavelet-type expansion of the process. As shown in Theorem 2 of Pipiras [1], under suitable conditions on the function ϕ, and with the notation $[x]$ for the integer part of $x \in \mathbb{R}$:

Wavelet-based approximation II: We have

$$\sup_{t\in K} |Z_\kappa(t) - Z_{\kappa,2}(j,t)| \leqslant C2^{-j\varepsilon} \to 0, \quad \text{a.s. as } j \to \infty, \tag{2.8}$$

where $K = \{t_1,\ldots,t_m\}$, C is a random variable, ε is any real such that $0 < 2\varepsilon < 4\kappa - 1$, and

$$Z_{\kappa,2}(j,t) = 2^{-2\kappa j} S^{(\kappa,2)}_{[2^j t],0}(j) \tag{2.9}$$

with $S^{(\kappa,2)}_{k,0}(j)$ defined by (2.4).

Approximation of a smooth function through its approximation coefficients is a standard result in the wavelet literature (see, for example, [15, p. 202], and also Proposition 2.1 in [16] in the case of fBm). Wavelet-based approximation II shows that this property holds for the wavelet-type expansion of fRm as well.

The convergence of the approximation coefficients found in the wavelet literature is, in fact, uniform in t belonging to a compact. We believe that the uniform convergence also holds in (2.8) but we lack the necessary tools to prove it at this time. For later reference and comparison, we nevertheless state the uniform convergence result as a conjecture. This conjecture is supported by our simulations in Section 5 below.

Wavelet-based approximation II (*Conjecture*): We have

$$\sup_{t\in K}|Z_\kappa(t)-Z_{\kappa,2}(j,t)|\to 0,\quad \text{a.s. as } j\to\infty, \tag{2.10}$$

where $Z_{\kappa,2}(j,t)$ is defined by (2.9) and K is compact subset of $\mathbb{R}$.

Observe also from (2.9) and (2.4) that, as mentioned in the Introduction, the second approximation $Z_{\kappa,2}$ has the simple form (1.6) with

$$Y_k=\xi_{J,k}^{(\kappa)}.$$

See Section 7 for a discussion of interest in using wavelet-based sequence $\xi_{J,k}^{(\kappa)}$. In particular, as argued in the next two sections, because of the underlying MRA structure, this sequence and hence the second approximation are extremely fast to generate.

Notation: In Sections 4–7, we shall also denote the two approximations $Z_{\kappa,i}(j,t)$ by

$$Z_{\kappa,i}(l,j,t),\quad i=1,2,$$

where $l\leqslant j$. The extra parameter l will refer to the scale at which the initial approximation to fRm is taken in simulation. See, in particular, Definitions (4.4) and (4.5).

3. Approximation coefficients and basis functions

Wavelet-based approximations I and II in Section 2 involve the approximation coefficients and the basis functions (2.7). We examine here these coefficients and functions, and show how they can be computed. We shall use the following notation. Let $x*y$ denote the *convolution* of two sequences x and y, and let the standard *upsample operation* $(\uparrow_2 x)$ insert zeros between the elements of a sequence x. For $s>0$, let also

$$u^{(s)}=f^{(s)}*u,\quad v^{(s)}=g^{(s)}*v, \tag{3.1}$$

where the filters $f^{(s)}=\{f_n^{(s)}\}$ and $g^{(s)}=\{g_n^{(s)}\}$ are defined through the z-transformations as

$$f^{(s)}(z)=(1+z^{-1})^s=\sum_{n=-\infty}^{\infty}f_n^{(s)}z^{-n},$$
$$g^{(s)}(z)=(1-z^{-1})^{-s}=\sum_{n=-\infty}^{\infty}g_n^{(s)}z^{-n}, \tag{3.2}$$

respectively, and u and v are the *low* and *high-pass filters* associated with the initial MRA corresponding to the scaling function ϕ and the wavelet ψ. The filters $u^{(s)}$ and $v^{(s)}$ are called *fractional filters*.

The next proposition shows that the sequence $\xi_{j,k}^{(\kappa)}$, $k\in\mathbb{Z}$, which defines the approximation coefficients through (2.4), can be computed by using the usual fast wavelet transform.

Proposition 3.1. *For $j\in\mathbb{Z}$ and $\kappa>0$, we have*

$$\xi_{j,\cdot}^{(\kappa)}=u^{(\kappa)}*(\uparrow_2\xi_{j-1,\cdot}^{(\kappa)})+v^{(\kappa)}*(\uparrow_2\varepsilon_{j-1,\cdot}). \tag{3.3}$$

Proof. The result (3.3) is implicit in Abry and Sellan [17], and follows from the results of Section 2 in Pipiras [16]. To the reader's convenience, we provide here a direct proof of this result by using z-transformations. By using (2.3), (3.1) and (3.2), and basic properties of z-transformations, we get that

$$\begin{aligned}&(u^{(\kappa)}*\uparrow_2\xi_{j-1,\cdot}^{(\kappa)}+v^{(\kappa)}*\uparrow_2\varepsilon_{j-1,\cdot})(z)\\&\quad=u^{(\kappa)}(z)\xi_{j-1,\cdot}^{(\kappa)}(z^2)+v^{(\kappa)}(z)\varepsilon_{j-1,\cdot}(z^2)\\&\quad=(1+z^{-1})^\kappa(1-z^{-2})^{-\kappa}u(z)\xi_{j-1,\cdot}(z^2)\\&\qquad+(1-z^{-1})^{-\kappa}v(z)\varepsilon_{j-1,\cdot}(z^2)\\&\quad=(1-z^{-1})^{-\kappa}(u(z)\xi_{j-1,\cdot}(z^2)+v(z)\varepsilon_{j-1,\cdot}(z^2))\\&\quad=(1-z^{-1})^{-\kappa}(u*\uparrow_2\xi_{j-1,\cdot}+v*\uparrow_2\varepsilon_{j-1,\cdot})(z).\end{aligned} \tag{3.4}$$

By using the properties of MRA, we have

$$\begin{aligned}&u*\uparrow_2\xi_{j-1,\cdot}+v*\uparrow_2\varepsilon_{j-1,\cdot}\\&\quad=\int_{\mathbb{R}}\{u*\uparrow_2\phi_{j-1,\cdot}(\xi)+v*\uparrow_2\psi_{j-1,\cdot}(\xi)\}\,\mathrm{d}B(\xi)\\&\quad=\int_{\mathbb{R}}\phi_{j,\cdot}(\xi)\,\mathrm{d}B(\xi)=\xi_{j,\cdot}.\end{aligned}$$

Hence, expression (3.4) becomes $(1-z^{-1})^{-\kappa}\xi_{j,\cdot}(z)=\xi_{j,\cdot}^{(\kappa)}(z)$. □

A computationally appealing feature of (3.3) is independence of the Gaussian detail coefficients $\varepsilon_{j,k}$. Another nice feature of (3.3) is related to the number of *zero moments* N of the orthogonal MRA associated with the low and high-pass filters u and v. It is known (see, for example, [15,18]) that, under mild conditions,

$$u(z)=(1+z^{-1})^N u_0(z),$$
$$v(z)=(1-z^{-1})^N v_0(z),$$

for some filters u_0 and v_0. Substituting these expressions into (3.1) and using (3.2), we get that

$$u^{(\kappa)}(z)=f^{(N+\kappa)}(z)u_0(z),$$
$$v^{(\kappa)}(z)=g^{(\kappa-N)}(z)v_0(z). \tag{3.5}$$

Observe that, as N becomes larger, the filters $f^{(N+\kappa)}$ and $g^{(\kappa-N)}$ decay much faster than the filters $u^{(\kappa)}$ and

$v^{(\kappa)}$. This shows, in particular, that increasing N makes the lengths of the filters $u^{(\kappa)}$ and $v^{(\kappa)}$, truncated at a fixed cutoff level, smaller as well. A more comprehensive discussion on the relations between the number of zero moments N and the length of the truncated filters $u^{(\kappa)}$ and $v^{(\kappa)}$, can be found in Pipiras [16].

The following is an elementary consequence of Proposition 3.1 and definition (2.4).

Computation of approximation coefficients: For $J \in \mathbb{Z}$, the approximation coefficients $S_{k,n}^{(\kappa,2)}(J)$ in (2.6) can be computed as follows. Compute the sequence $\xi_{J,k}^{(\kappa)}$, $k \in \mathbb{Z}$, from $\xi_{L,k}^{(\kappa)}$, $k \in \mathbb{Z}$, and independent $\mathcal{N}(0,1)$ random variables $\varepsilon_{j,k}$, $k \in \mathbb{Z}$, $j = L, 1, \ldots, J-1$, by using (3.3) together with (3.5), where $L<J$ is a fixed integer. Use the obtained sequence to form the approximation coefficients through (2.4).

Computation of basis functions: We compute the basis functions $\Phi_{\kappa,n}^{(2)}$ in (2.6) by discretizing the integral in the definition (2.2). The function $\phi_{\kappa,\Delta}$ in the integral is computed by using the fast Fourier transform as the inverse of the Fourier transform (2.1).

In the left plot of Fig. 1 below, we provide the plot of the scaling function ϕ corresponding to the Daubechies MRA with $N = 6$ zero moments and the function $\phi_{\kappa,\Delta}$ defined from the function ϕ by (2.1) with $\kappa = 0.35$. The scale function ϕ has a compact support $[0, 11]$ but the function $\phi_{\kappa,\Delta}$ is supported on $[0, \infty)$. Fig. 1 shows, however, that the function $\phi_{\kappa,\Delta}$ decays relatively fast and its shape resembles closely that of the function ϕ. In the right plot of Fig. 1 below, we plot the functions $\Phi_{\kappa,n}^{(2)}$ defined from the function $\phi_{\kappa,\Delta}$ by (2.2) with $n = -2, -1, 0, 1, 2$. As expected from the definition (2.2), these functions are most prevalent when $n = 0$, and they become less significant as $|n|$ increases.

Choosing the multiresolution: Theoretically, most common MRAs could be used in the construction above. In this work, we consider only the Daubechies MRAs with N zero moments. These MRAs are widely used and convenient to deal with because of compact time supports. In particular, for Daubechies MRAs, the related filters u_0, v_0 appearing in (3.5) are readily available from Daubechies [15, p. 196] and are finite. This is convenient in practice when computing the fractional filters $u^{(\kappa)}, v^{(\kappa)}$ according to (3.5).

4. Practical implementation

The practical implementations of the wavelet based fRm approximations I and II can be performed through the following algorithms.

Input parameters: The parameters entering the wavelet-based synthesis of fRm are the following ones:

- Choose the parameter $\kappa \in (\frac{1}{4}, \frac{1}{2})$ defining fRm.
- Choose the multiresolution (MRA) orthogonal wavelet basis. In the present implementation, we work with the orthogonal [15] wavelets, parameterized by their number of zero moments N.

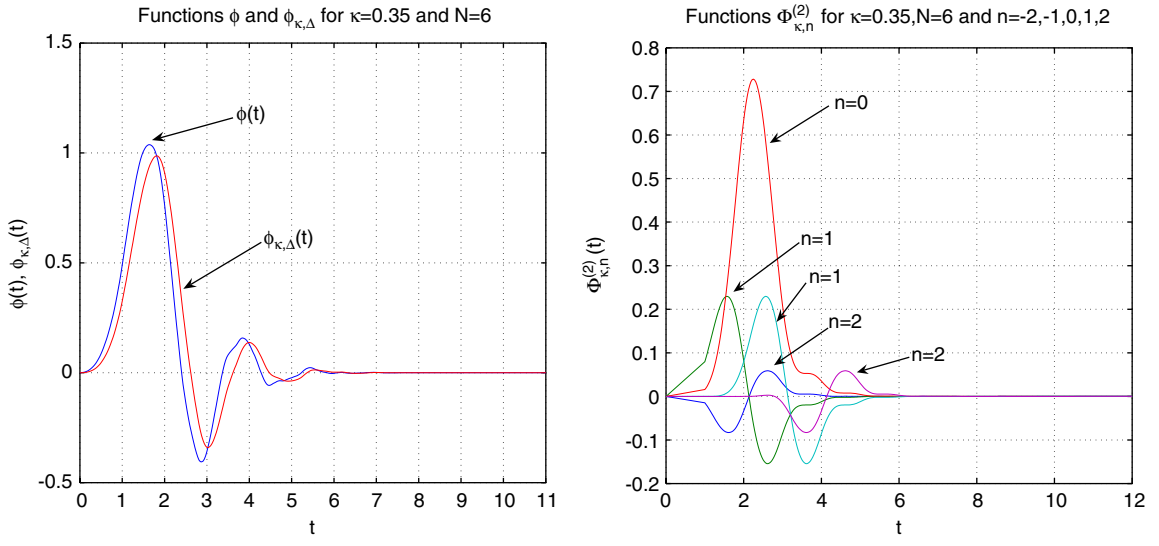

Fig. 1. Daubechies ($N = 6$) scaling function ϕ; functions $\phi_{\kappa,\Delta}$ and $\Phi_{\kappa,n}^{(2)}$ defined by (2.1) and (2.2).

- Choose the time duration $[0, T]$ of the synthesis of fRm. For simplicity, this will be chosen as
$$T = 2^M. \tag{4.1}$$
- Choose the scale
$$2^{-J} \tag{4.2}$$
at which one desires to obtain the wavelet-based approximation of fRm. In other words, the approximation of fRm is obtained at the time points $0, 2^{-J}, 2\cdot 2^{-J}, \ldots, 2^{M+J}\cdot 2^{-J} (= T)$ and hence that its length is $2^{M+J}+1$. We will refer to 2^{-J} in (4.2) as the final approximation scale.
- Choose a parameter L such that
$$-M \leqslant L \leqslant J. \tag{4.3}$$

This parameter is discussed below in this section, and its role is studied in Section 6.

Implementing wavelet-based approximation II: We implement the wavelet-based approximation II through the following steps:

- First, compute the fractional filters $u^{(\kappa)}$ and $v^{(\kappa)}$ by using (3.5). Since these filters are infinite, truncate them at a specified cutoff level δ. Let r denote the maximum length of the truncated filters $u^{(\kappa)}$ and $v^{(\kappa)}$.
- Second, generate an initial FARIMA$(0, \kappa, 0)$ sequence $\xi^{(\kappa)}$ of length $r + 2^{M+L}$. In the current implementation, we chose to use the Circular Matrix Embedding method (see [19] or a nice review by Bardet et al. [20]).
- Third, apply the fast wavelet transform (3.3) to the initial FARIMA sequence $\xi^{(\kappa)}$ recursively $J - L$ times to obtain $r + 2^{M+J}$ observations of another FARIMA$(0, \kappa, 0)$ sequence $\widetilde{\xi}^{(\kappa)}$.
- Fourth, in view of (2.4), form the partial sums
$$\begin{aligned}\widetilde{S}^{(\kappa,2)}_{k,0} &= \sum_{0<i\leqslant k} ((\widetilde{\xi}^{(\kappa)}_i)^2 - E(\widetilde{\xi}^{(\kappa)}_i)^2)\\ &= \sum_{0<i\leqslant k}\left((\widetilde{\xi}^{(\kappa)}_i)^2 - \frac{\Gamma(1-2\kappa)}{(\Gamma(1-\kappa))^2}\right),\\ &\quad k = 0, \ldots, 2^{M+J},\end{aligned}$$
where we used the formula (13.2.8) in Brockwell and Davis [14].
- Fifth, use the sequence
$$Z_{\kappa,2}(L, J, t = k2^{-J}) = C_\kappa 2^{-2\kappa J}\widetilde{S}^{(\kappa,2)}_{k,0} \quad \text{with}$$
$$C_\kappa = \frac{\Gamma(\kappa)\Gamma(1-\kappa)\sqrt{(4\kappa-1)\kappa}}{\Gamma(1-2\kappa)} \tag{4.4}$$
for the wavelet-based approximation II of fRm $Z_\kappa(t)$ at the time points $t = 0, 2^{-J}, 2\cdot 2^{-J}, \ldots, 2^M$.

Comments: A number of comments are in order:

The maximum length r of the filters $u^{(\kappa)}$ and $v^{(\kappa)}$ turns out to be surprisingly small for large enough number of zero moments of the chosen underlying orthogonal MRA [16].

The length $r+1$ is the smallest length which makes the use of the (3.3) possible when taking into account the boarder effect. Let us note that this corresponds to the choice $L = -M$. The impact of the choice of the initial FARIMA sequence and hence of the parameter L is detailed in Section 6.

Observe that $r + 2^{M+J}$ is the length of the FARIMA sequence which appears after applying the scheme (3.3) recursively $J - L$ times to the initial FARIMA sequence of length $r + 2^{M+L}$ while taking into account the boarder effect (see also Section 4 in [16]).

The constant C_κ in (4.4) ensures that $EZ_\kappa(1)^2 = 1$ in the limit $J \to \infty$. This can be deduced from Theorem 2 and relations (1.2), (1.3) of Pipiras [1]. It can also be obtained directly by assuming that $E(2^{-2\kappa J}\widetilde{S}^{(\kappa,2)}_{2^J,0})^2 \sim C_\kappa^{-2}$, as $J \to \infty$, and computing the variance using the well-known formula $EH_2(X)H_2(Y) = 2(EXY)^2$ for a Gaussian zero mean vector (X, Y) and the function $H_2(x) = x^2 - 1$ (see, for example, (1.11) in [7], p. 29). The normalization $2^{2\kappa J}$ is consistent with the (2κ)-self-similarity of fRm.

The choice of J and M is subjective but it affects the error of the approximation of fRm (see Section 6).

Implementing wavelet-based approximation I: Using (2.6) with $j = J$ at the time points $t = k2^{-J}$ with $k = 0, 1, \ldots, 2^{M+J}$, leads to the approximation
$$2^{-2\kappa J}\sum_{n=-\infty}^{\infty}\sum_{p=-\infty}^{\infty}\Phi^{(2)}_{\kappa,n}(k-p)S^{(\kappa,2)}_{p,n}(J) - z^{(J)}_0.$$
Observe that $\Phi^{(2)}_{\kappa,n}$ involves only its values at the integer points. Since $\Phi^{(2)}_{\kappa,n}(z) = 0$ for $z \leqslant 0$ (see (2.2) and note that $\phi_{\kappa,A}(v) = 0$ for $v \leqslant 0$), we truncate the series above as
$$Z_{\kappa,1}(L, J, t = k2^{-J}) = 2^{-2\kappa J}\sum_{n=-N_0}^{N_0}\sum_{p=k-K_0}^{k}\Phi^{(2)}_{\kappa,n}(k-p)S^{(\kappa,2)}_{p,n}(J) - z^{(J)}$$

$$= 2^{-2\kappa J} \sum_{n=-N_0}^{N_0} \sum_{q=0}^{K_0} \Phi^{(2)}_{\kappa,n}(q) S^{(\kappa,2)}_{k-q,n}(J) - z^{(J)}. \quad (4.5)$$

The practical implementation of this approximation consists of the following steps:

- First, the sequence $S^{(\kappa,2)}_{k,n}(J)$ in (4.5) is computed as for the wavelet-based approximation II using steps 1–4.
- Second, the function values $\Phi^{(2)}_{\kappa,n}(q)$ are obtained as explained at the end of Section 3.
- Third, since we expect the function $\phi_{\kappa,\Delta}$ in (2.2) to resemble the function ϕ with its support on $[0, 2N-1]$ (see Fig. 1), we choose $N_0 = N$ and $K_0 = 2N$ in the approximation (4.5).

Sequence of approximations: Wavelet-based approximations I and II can be formed not only after the $J-L$ applications of the fast wavelet-transform (3.3) but also with the initial FARIMA sequence and after *each* of the $J-L$ applications of (3.3). We can thus obtain approximations I and II as sequences of approximations at consecutive, finer and finer, scales 2^{-j}, $L \leqslant j \leqslant J$, that is, $\{Z_{\kappa,i}(L, j, t = k2^{-j}),\ k = 0, 1, \ldots, 2^{M+J}\}_{L \leqslant j \leqslant J}$, $i = 1, 2$. Note that the length of the approximations at scale 2^{-j} is $2^{M+j} + 1$.

The approximations $Z_{\kappa,i}(L, L, t = k2^{-L})$, $k = 0, 1, \ldots, 2^{M+L}$, of length $2^{M+L} + 1$ will be referred to as the initial approximations. The scale

$$2^{-L}, \quad (4.6)$$

where $-M \leqslant L \leqslant J$, will be referred to as the initial approximation scale.

For example, Fig. 2 depicts consecutive wavelet-based approximations II to fRm Z_κ, with $\kappa = 0.35$, $N = 10$, $M = 0$ (or $[0, T] = [0, 1]$), $J = 17$ and $L = -M = 0$. We selected $\delta = 10^{-6}$ for the truncation level of the fractional filters and the length r of the truncated filters was 23.

5. Uniform convergence and equivalence of the two approximations

In this section, without loss of generality, we restrict the exposition to the case $M = 0$, i.e., $T = 1, K = [0, 1]$ and $L = -M = 0$. Fig. 2 nicely illustrates the convergence of the approximations to fRm. We can use the underlying algorithm to provide empirical evidence that both wavelet-based

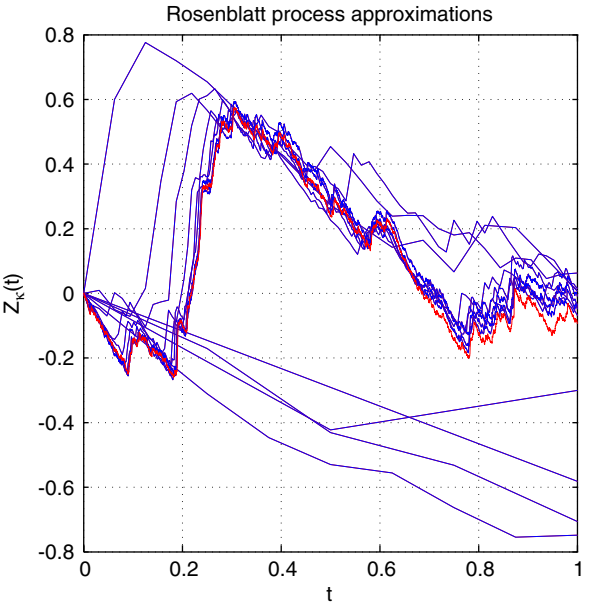

Fig. 2. Consecutive wavelet-based approximations II to fRm Z_κ with $\kappa = 0.35$.

approximations I and II converge almost surely and uniformly on compact intervals, and that they are asymptotically equivalent. For this, define the random variables

$$C^\kappa_i(j) = \sup_{t \in [0,1]} |Z_{\kappa,i}(0, j, t) - Z_\kappa(t)|, \quad (5.1)$$

$$D^\kappa_i(j) = \sup_{t \in [0,1]} |Z_{\kappa,i}(0, j+1, t) - Z_{\kappa,i}(0, j, t)|, \quad (5.2)$$

$$F^\kappa(j) = \sup_{t \in [0,1]} |Z_{\kappa,1}(0, j, t) - Z_{\kappa,2}(0, j, t)|, \quad (5.3)$$

where $i = 1, 2$, $0 \leqslant j \leqslant J$.

Note that, unlike $C^\kappa_i(j)$, the variables $D^\kappa_i(j)$ and $F^\kappa(j)$ are observable. In practice, for simplicity, we replace the suprema over $t \in [0, 1]$ by the suprema over $t = 0, 2^{-(j+1)}, 2 \cdot 2^{-(j+1)}, \ldots, 1$, for $D^\kappa_i(j)$ and the suprema over $t = 0, 2^{-j}, 2 \cdot 2^{-j}, \ldots, 1$, for $F^\kappa(j)$. Note also that, ignoring truncation of the series in (4.5),

$$\begin{aligned} C^\kappa_1(j) &= \lim_{j' \to \infty} \sup_{t \in [0,1]} |Z_{\kappa,1}(0, j, t) - Z_{\kappa,1}(0, j', t)| \\ &\leqslant \lim_{j' \to \infty} \sum_{p=j}^{j'-1} \sup_{t \in [0,1]} |Z_{\kappa,1}(0, p+1, t) \\ &\quad - Z_{\kappa,1}(0, p, t)| \\ &= \sum_{p=j}^{\infty} D^\kappa_1(p). \end{aligned} \quad (5.4)$$

Hence, we may get a bound on the variable $C_1^\kappa(j)$ from $D_1^\kappa(p)$, $p \geqslant j$. We know from (2.5) that, ignoring truncation of the series, $C_1^\kappa(j)$ and $D_1^\kappa(j)$ converge to 0 almost surely, as $j \to \infty$. We conjectured in (2.10) that the same result holds for $C_2^\kappa(j)$ and $D_2^\kappa(j)$. We therefore, expect that (5.4) holds for $C_2^\kappa(j)$ and $D_2^\kappa(j)$ as well.

In Fig. 3, we provide ten realizations and boxplots of the distributions of $\ln(D_i^\kappa(j))$, $i = 1, 2$, and $\ln(F^\kappa(j))$, $\kappa = 0.35$, as functions of $j = 0, \ldots, 18$. The boxplots are based on 1000 independent realizations. The other simulation parameters are the same as those for Fig. 2. These plots suggest that $D_i^\kappa(j)$, $i = 1, 2$, and $F^\kappa(j)$ converge almost surely, uniformly on $[0, 1]$ and exponentially fast to 0 as $j \to \infty$. By using (5.4), we expect that the same holds for $C_i^\kappa(j)$, $i = 1, 2$. This observation is consistent with (2.5) in the case of $C_1^\kappa(j)$. It also supports the conjecture made at the end of Section 2 in the case of $C_2^\kappa(j)$ and the fact that the two approximations are asymptotically equivalent. Observe from Fig. 3 that the approximation $Z_{\kappa,2}(0, j, t)$ exhibits more stability (less variance) than $Z_{\kappa,1}(0, j, t)$ as j becomes large.

The convergence of both approximations $Z_{\kappa,i}(0, j, t)$, $i = 1, 2$, appears slower and less stable (more variant) when $\kappa \in (\frac{1}{4}, \frac{1}{2})$ is closer to $\frac{1}{4}$. We illustrate this in Fig. 4 where ten realizations and boxplots of $\ln(D_i^\kappa(j))$, $i = 1, 2$, and $\ln(F^\kappa(j))$ are provided for $\kappa = 0.28$. The convergence appears particularly slow and unstable for wavelet-based approximation I. Observe also that the decay of $\ln(F^\kappa(j))$ appears surprisingly little affected.

6. On the practical use of wavelet-based simulation

We discuss here several practical issues related to the wavelet-based synthesis of fRm: the choice of initial scale 2^{-L} in (4.6), the joint selection of M and J, and the synthesis of fRm on the integer grid.

Choice of initial scale 2^{-L}: Suppose that M and J are fixed in (4.1) and (4.2). As mentioned in Section 4, the shortest possible initial FARIMA sequence in the wavelet-based simulation of fRm has length $r + 1$. This corresponds to the choice $L = -M$ or the initial scale $2^{-L} = 2^M$ or the initial approximation of length $2^0 + 1$. However, starting with a longer initial FARIMA sequence, we can use instead an arbitrary initial scale 2^{-L} in (4.6) with $-M \leqslant L \leqslant J$ in (4.3). We now want to address questions such as: Does it matter what initial scale (4.6) with (4.3) is used? Alternatively, does it matter how long the initial approximation is taken?

In terms of approximation errors, these questions can be inquired through the variables

$$C_{K,i}^\kappa(L, j) = \sup_{t \in K} |Z_{\kappa,i}(L, j, t) - Z_\kappa(L, t)|, \tag{6.1}$$

$$D_{K,i}^\kappa(L, j) = \sup_{t \in K} |Z_{\kappa,i}(L, j+1, t) - Z_{\kappa,i}(L, j, t)|, \tag{6.2}$$

where $K \subset \mathbb{R}$, $i = 1, 2$, $L \leqslant j \leqslant J$, $Z_{\kappa,i}(L, j, t)$ is a wavelet-based approximation at scale 2^{-j} obtained in practice starting with approximation at the initial scale 2^{-L}, and $Z_\kappa(L, t) = \lim_{J \to \infty} Z_{\kappa,1}(L, J, t)$ is the corresponding limiting Rosenblatt process. When $K = [0, 1]$ and $L = 0$, the variables (6.1) and (6.2) are those in (5.1) and (5.2).

The following result shows that approximation errors (6.1) and (6.2) are not affected by the initial scale. The result is analogous to Proposition 3.1 in Pipiras [21].

Proposition 6.1. *For* $i = 1, 2$, $L_0 = \max(L_1, L_2)$, *we have*

$$\{C_{K,i}^\kappa(L_1, j)\}_{j \geqslant L_0} \stackrel{d}{=} \{C_{K,i}^\kappa(L_2, j)\}_{j \geqslant L_0},$$

$$\{D_{K,i}^\kappa(L_1, j)\}_{j \geqslant L_0} \stackrel{d}{=} \{D_{K,i}^\kappa(L_2, j)\}_{j \geqslant L_0}. \tag{6.3}$$

(*When* $i = 2$, *the first relation of* (6.3) *holds in fact under Conjecture* (2.10).)

Proof. The results (6.3) follow from the identity

$$\{Z_{\kappa,i}(L_1, j, t),\ j \geqslant L_0, t \in \mathbb{R}\} \stackrel{d}{=} \{Z_{\kappa,i}(L_2, j, t),\ j \geqslant L_0, t \in \mathbb{R}\}. \tag{6.4}$$

To understand (6.4), suppose that $L_1 < L_2$. Observe that the processes $Z_{\kappa,i}(L_2, j, t)$, $j \geqslant L_0$, are defined starting with an initial FARIMA$(0, \kappa, 0)$ sequence $\{\xi_{L_2,n}^{(\kappa)}\}$. The processes $Z_{\kappa,i}(L_1, j, t)$, $j \geqslant L_0$, can be defined in the same way but starting with a sequence

$$\{\xi_{L_2,n}^{(\kappa)}(L_1)\} \tag{6.5}$$

obtained from an initial FARIMA$(0, \kappa, 0)$ sequence $\{\xi_{L_1,n}^{(\kappa)}\}$ after recursively applying the fast wavelet transform (3.3). The identity (6.4) follows since (6.5) is also a FARIMA$(0, \kappa, 0)$ sequence. □

The second result of (6.3) can be confirmed by simulation. In Fig. 5 below, we provide boxplots of the distributions of $D_{[0,1],2}^\kappa(L, J)$ with $J = 11$ and $J = 19$ as functions of $L = 0, 1, \ldots, J - 1$. For $J = 19$, for example, each value of the error $D_{[0,1],2}^\kappa(L, 19)$ is computed from the wavelet-based

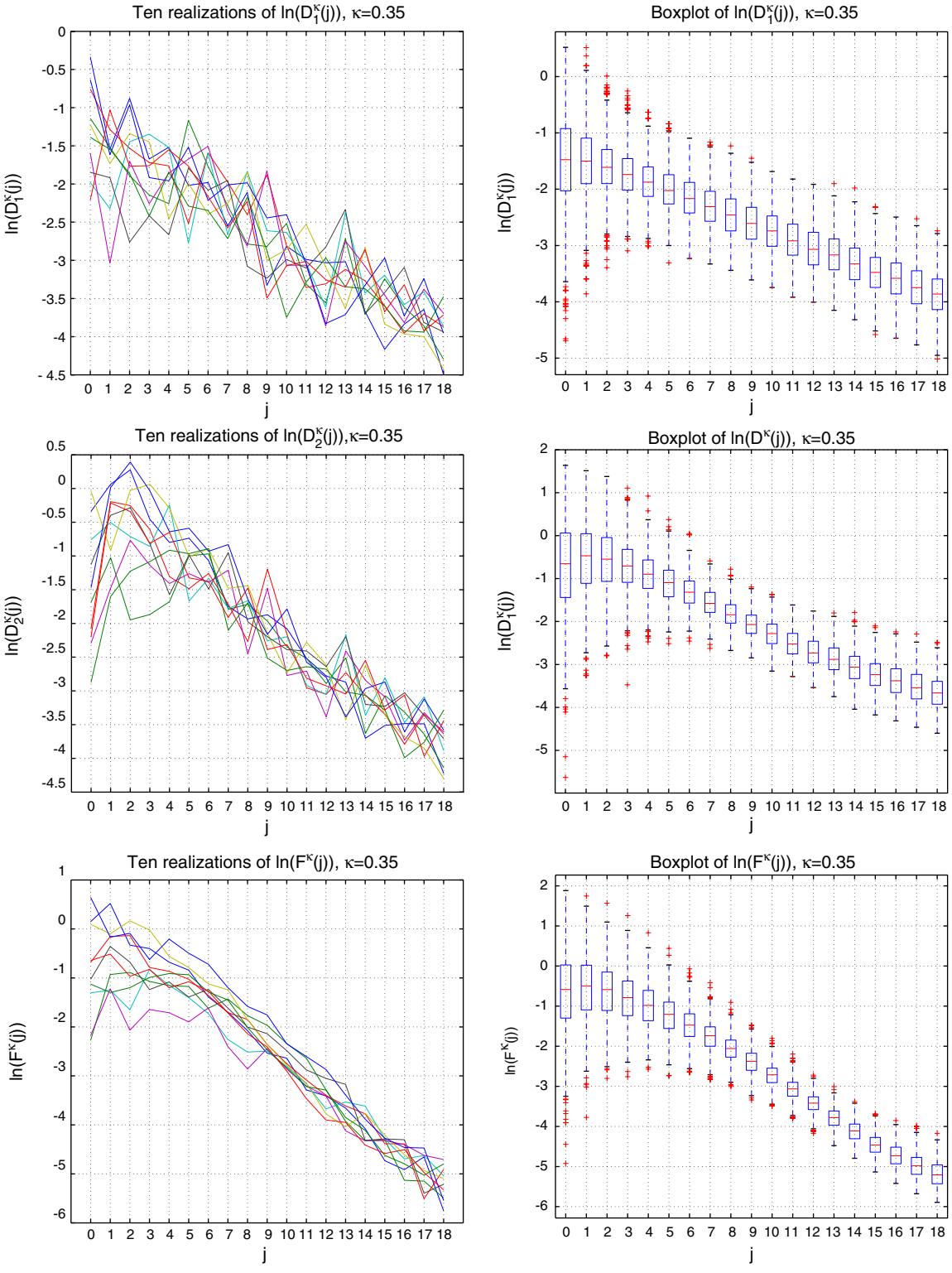

Fig. 3. 10 realizations and boxplots of the variables $\ln(D_1^\kappa(j))$, $\ln(D_2^\kappa(j))$ and $\ln(F^\kappa(j))$ with $\kappa = 0.35$ discussed in Section 5.

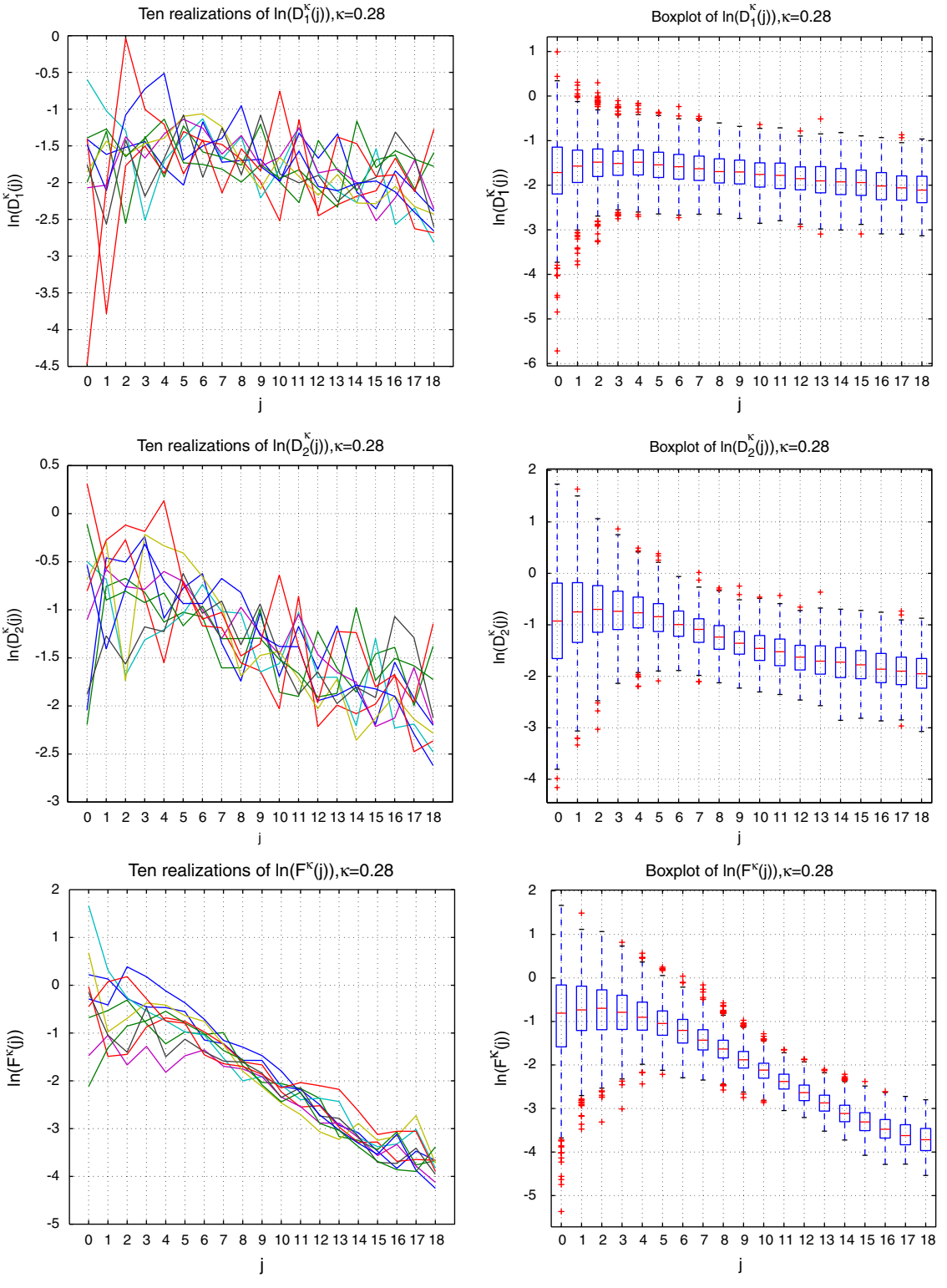

Fig. 4. 10 realizations and boxplots of the variables $\ln(D_1^\kappa(j))$, $\ln(D_2^\kappa(j))$ and $\ln(F^\kappa(j))$ with $\kappa = 0.28$ discussed in Section 5.

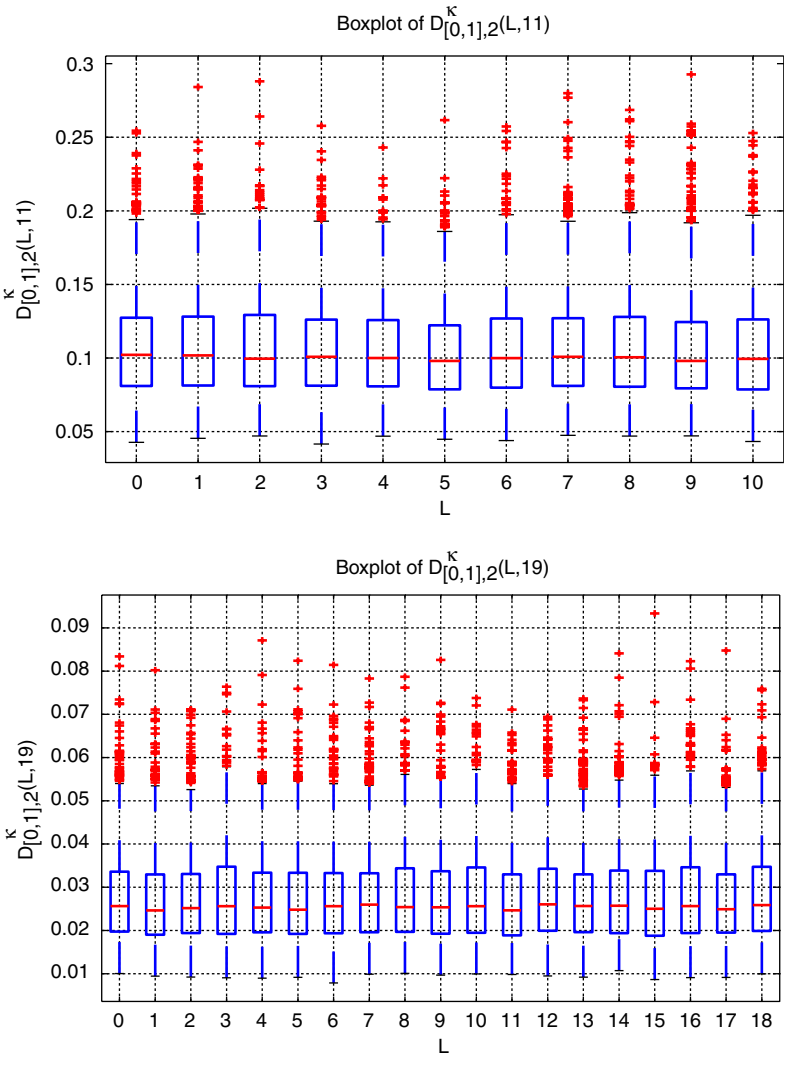

Fig. 5. Boxplots of the variables $D^{\kappa}_{[0,1],2}(L,11)$ and $D^{\kappa}_{[0,1],2}(L,19)$ discussed in Section 6.

approximations $Z_{\kappa,2}(L,20,t)$ of length $2^{20}+1$ and $Z_{\kappa,2}(L,19,t)$ of length $2^{19}+1$. We chose $J=11$ and $J=19$ to indicate that the conclusions are not affected by the length of the final approximation and by the number of times that the fast wavelet transform (3.3) is performed. The parameters in simulation are those as for Figs. 2 and 3, in particular, $\kappa=0.35$. Analogous observations can be made in the case $i=1$.

Joint selection of M and J: In practice, the choice of final scale 2^{-J} and simulation interval $[0,2^M]$ is subjective. The same final wavelet-based approximation of length $2^{J+M}+1$ at times $0,2^{-J}$, $2\cdot 2^{-J},\ldots,2^M$ can be used as approximation at times $0,2^{-(J-J')},2\cdot 2^{-(J-J')},\ldots,2^{M+J'}$ for any $J'\in\mathbb{Z}$, that is, at scale $2^{-(J-J')}$ and on simulation interval $[0,2^{M+J'}]$. What difference does this make?

The difference is in the error of approximation. The next result is analogous to Proposition 6.1 in Pipiras [21].

Proposition 6.2. *We have for $J,J'\in\mathbb{Z}$, $i=1,2$,*

$$C^{\kappa}_{K,i}(0,J)\overset{d}{=}2^{-2\kappa J'}C^{\kappa}_{2^{J'}K,i}(0,J-J'),$$
$$D^{\kappa}_{K,i}(0,J)\overset{d}{=}2^{-2\kappa J'}D^{\kappa}_{2^{J'}K,i}(0,J-J'). \tag{6.6}$$

In particular,

$$C^{\kappa}_{[0,2^M],i}(0,J)\overset{d}{=}2^{2\kappa M}C^{\kappa}_{[0,1],i}(0,J+M),$$
$$D^{\kappa}_{[0,2^M],i}(0,J)\overset{d}{=}2^{2\kappa M}D^{\kappa}_{[0,1],i}(0,J+M). \tag{6.7}$$

Proof. Consider, for example, the case of $C^{\kappa}_{K,1}$. By using (2.6) and the (2κ)-self-similarity of fRm, we obtain that

$$\begin{aligned} C^{\kappa}_{K,1}(0,J) &= \sup_{2^{-J'}t\in K} |Z_{\kappa,1}(J,2^{-J'}t) - Z_{\kappa}(2^{-J'}t)| \\ &\stackrel{d}{=} 2^{-2\kappa J'} \sup_{2^{-J'}t\in K} |Z_{\kappa,1}(J-J',t) - Z_{\kappa}(t)| \\ &= 2^{-2\kappa J'} \sup_{t\in 2^{J'}K} |Z_{\kappa,1}(J-J',t) - Z_{\kappa}(t)| \\ &= 2^{-2\kappa J'} C^{\kappa}_{2^{J'}K,1}(0,J-J'). \qquad \square \end{aligned}$$

Suppose as above that the final approximation is at scale 2^{-J} and on simulation interval $[0,2^M]$. If $J'>0$, relation (6.6) shows that using the same approximation at larger scale $2^{-(J-J')}$ and on larger simulation interval $[0,2^{M+J}]$, will increase the approximation error $2^{2\kappa J'}$ times. If $J'<0$, the approximation error will decrease $2^{2\kappa J'}$ times. Relation (6.7) shows that approximation errors for arbitrary simulation intervals $[0,2^M]$ can be deduced from those for the simulation interval $[0,1]$. In this sense, Figs. 3 and 4 carry information about approximation errors on arbitrary intervals. These figures can therefore guide a user in choosing a final scale for a targeted approximation error.

Approximation of fRm on the integer grid: From the arguments developed in the paragraph above, it is clear that choosing $J=0$ so as to obtain an approximation on the integer grid $0,1,\ldots,2^M$ leads to large approximation errors. This can be seen from the relation

$$D^{\kappa}_{[0,2^M],i}(0,0) \stackrel{d}{=} 2^{2\kappa M} D^{\kappa}_{[0,1],i}(0,M), \tag{6.8}$$

which is a consequence of (6.7). Even though the errors $D^{\kappa}_{[0,1],i}(0,M)$ decrease with M (Figs. 3 and 4), they become large when multiplied by $2^{2\kappa M}$.

To obtain a more accurate approximation on the integer grid, it is necessary to generate wavelet-based approximation on $[0,2^M]$ at a finer final scale 2^{-J}, $J>0$, and then retain only those values corresponding to integer times. In this case, the approximation error of full approximation is $D^{\kappa}_{[0,2^M],i}(0,J) \geqslant D^{\kappa}_{\{0,1,\ldots,2^M\},i}(0,J)$. Observe that $D^{\kappa}_{[0,2^M],i}(0,J)$ is smaller than (6.8) in view of (6.7). The discussion above can guide a user in choosing J for a targeted approximation error. Retaining approximation values at integer times amounts to performing a downsampling of the wavelet-based approximation. Downsampling thus reduces approximation errors.

7. Usefulness of wavelet-based synthesis

We argued in Section 6 that the approximation error does not depend on initial scale 2^{-L} in the wavelet-based synthesis of fRm. When final scale 2^{-J} is fixed, this means, in particular, that we may as well take the initial scale 2^{-L} to be the final scale 2^{-J} itself. In this case, there is no need to use the fast wavelet transform algorithm (3.3). In other words, using the simple-minded approximation in (1.5) given by

$$2^{-2\kappa J} \sum_{k=1}^{[2^J t]} (X_k^2 - 1), \tag{7.1}$$

where $\{X_k\}$ is a Gaussian FARIMA$(0,\kappa,0)$ sequence generated, for example, by the Circulant Matrix Embedding method, is equally good as using the wavelet-based approximation $Z_{\kappa,2}(L,J,t)$ with some $L<J$. This is perhaps not that surprising because $Z_{\kappa,2}(L,J,t)$ are also defined by (7.1) where $\{X_k\}$ is a special FARIMA sequence generated by using wavelets.

If one can use a simple-minded approximation (7.1), why is the wavelet-based synthesis of fRm useful? This question was addressed by Pipiras [21] in the case of fractional Brownian motion. The reasons for interest provided in that work are relevant here as well. Some other reasons are specific to the case of fRm. The wavelet-based synthesis of fRm is useful for at least the following reasons:

- First, it provides approximations which converge to fRm almost surely and uniformly on compact intervals. The approximation (7.1) is identical to $Z_{\kappa,2}(L,J,t)$ but only on average (in distribution). By increasing J, we can in principle make $Z_{\kappa,2}(L,J,t)$ arbitrarily close to fRm almost surely. This is not the case for the approximation (7.1). The almost sure convergence is particularly important in the case of fRm because exact simulation of the process is not available. It can also be used to visualize the convergence to fRm as illustrated in Fig. 2.
- Second, the wavelet-based synthesis provides information on the approximation error when using other simulation methods. For example, when using (7.1) at some fixed scale 2^{-J}, the approximation error is the same (in distribution) as that when using the approximations $Z_{\kappa,2}(L,J,t)$. The approximation error of the

latter can be explored through Figs. 3 and 4 type plots.

- Third, the wavelet-based synthesis is computationally fast. Modulo truncation of the fractional filters, the wavelet-based synthesis is of the order $O(T)$, where T is the length of a wavelet-based approximation of fRm. Truncation of the fractional filters refers here to the discussion around (3.5). When the number of zero moments N is larger, the lengths of the fractional filters $u^{(\kappa)}$ and $v^{(\kappa)}$, truncated at a negligible cutoff level, are surprisingly small. Using these finite, truncated filters within (3.3), one can generate the sequence $\xi_{j,k}^{(\kappa)}$ at the speed of fast wavelet transform. Since T random variables $\xi_{j,k}^{(\kappa)}$ are needed to obtain the approximation $Z_{\kappa,2}$ of fRm of length T, its computational cost is of the order of that of a fast wavelet transform, that is, $O(T)$.

8. Conclusions and perspectives

In the present work, we studied two wavelet-based approximations for the Rosenblatt processes. As detailed in Section 4, approximation I in (2.5) has a stronger mathematical foundation than approximation II in (2.8). However, we saw in Section 5 from numerical simulations that both approximations turn out to be equivalent in terms of uniform convergence. Also, we note from Sections 6 and 7 that the issues regarding their use and usefulness are identical. Since approximation II is significantly simpler and has a lower computational cost, we would recommend to use it in practice.

The use of a well-controlled and well-understood algorithm to synthesize the Rosenblatt processes is of key importance to the analysis of scaling phenomena. Indeed, these finite variance, non-Gaussian, self-similar processes with stationary increments provide a relevant alternative to both fractional Brownian motions and multifractal processes for the modeling of empirical data with scaling properties. They could also prove very useful for the analysis of scaling parameter estimation performance and for the study of self-similarity versus multifractal hypothesis testing.

Matlab routines implementing both approximations as well as the uniform convergence discussion and the synthesis (with detailed explanations) of the basis functions in (2.7) are available upon request.

Acknowledgements

We would like to thank an anonymous referee for carefully reading the original manuscript and for suggestions.

References

[1] V. Pipiras, Wavelet-type expansion of the Rosenblatt process, J. Fourier Anal. Appl. 10 (6) (2004) 599–634.
[2] D. Nualart, The Malliavin Calculus and Related Topics, Springer, New York, 1995.
[3] P. Embrechts, M. Maejima, Self Similar Processes, Academic Press, New York, 2003.
[4] G. Samorodnitsky, M.S. Taqqu, Stable Non-Gaussian Processes: Stochastic Models with Infinite Variance, Chapman & Hall, New York, London, 1994.
[5] M. Rosenblatt, Independence and dependence, in: Proceedings of the Fourth Berkeley Symposium on Mathematics, Statistics and Probability, vol. II, University of California Press, Berkeley, CA, 1961, pp. 431–443.
[6] M.S. Taqqu, Convergence of integrated processes of arbitrary Hermite rank, Z. Wahr. verwandt. Geb. 50 (1979) 53–83.
[7] R.L. Dobrushin, P. Major, Non-central limit theorems for non-linear functions of Gaussian fields, Z. Wahr. verwandt. Geb. 50 (1979) 27–52.
[8] R. Fox, M.S. Taqqu, Non-central limit theorems for quadratic forms in random variables having long-range dependence, Ann. Probab. 13 (1985) 428–446.
[9] J.M.P. Albim, A note on the Rosenblatt distributions, Statist. Probab. Lett. 40 (1) (1998) 83–91.
[10] J. Beran, Statistics for long-memory processes, in: Monographs on Statistics and Applied Probability, vol. 61, Chapman & Hall, New York, 1994.
[11] P. Doukhan, G. Oppenheim, M.S. Taqqu (Eds.), Theory and Applications of Long-Range Dependence, Birkhäuser Boston Inc., Boston, MA, 2003.
[12] N.H. Bingham, C.M. Goldie, J.L. Teugels, Regular Variation, Cambridge University Press, Cambridge, 1987.
[13] M.A. Arcones, Limit theorems for non-linear functionals of a stationary Gaussian sequence of vectors, Ann. Probab. 22 (1994) 2242–2274.
[14] P.J. Brockwell, R.A. Davis, Time Series: Theory and Methods, second ed., Springer, New York, 1991.
[15] I. Daubechies, Ten Lectures on Wavelets, CBMS-NSF series, vol. 61, SIAM, Philadelphia, PA, 1992.
[16] V. Pipiras, Wavelet-based simulation of fractional Brownian motion revisited, Appl. Comput. Harmonic Anal. 19 (1) (2005) 49–60.
[17] P. Abry, F. Sellan, The wavelet-based synthesis for the fractional Brownian motion proposed by F. Sellan and Y. Meyer: Remarks and fast implementation, Appl. Comput. Harmonic Anal. 3(4) (1996) 377–383.
[18] S. Mallat, A Wavelet Tour of Signal Processing, Academic Press, Boston, 1998.
[19] C.R. Dietrich, G.N. Newsam, Fast and exact simulation of stationary Gaussian processes through circulant embedding of the covariance matrix, SIAM J. Sci. Comput. 18 (4) (1997) 1088–1107.

[20] J.-M. Bardet, G. Lang, G. Oppenheim, A. Philippe, M.S. Taqqu, Generators of long-range dependent processes: a survey, in: P. Doukhan, G. Oppenheim, M.S. Taqqu (Eds.), Long-Range Dependence: Theory and Applications, Birkhäuser, Boston, 2003, pp. 579–623.

[21] V. Pipiras, On the usefulness of wavelet-based simulation of fractional Brownian motion, 2003, Preprint. Available at ⟨http://www.stat.unc.edu/faculty/pipiras/⟩